Cancer Immunol Immunother (2012) 61:855–864
DOI 10.1007/s00262-011-1146-8

ORIGINAL ARTICLE

Calreticulin as a potential diagnostic biomarker for lung cancer

Rongrong Liu · Jiuyu Gong · Jun Chen · Qi Li · Chaojun Song · Jian Zhang · Yongming Li · Zhijia Liu · Yun Dong · Lihua Chen · Boquan Jin

Received: 2 September 2011 / Accepted: 26 October 2011 / Published online: 15 November 2011

Abstract Calreticulin (CRT) is an endoplasmic reticulum luminal Ca^{2+}-binding chaperone protein. By immunizing mice with recombinant fragment (rCRT/39-272), six clones of monoclonal antibodies (mAbs) were generated and characterized. Based on these mAbs, a microplate chemiluminescent enzyme immunoassay (CLEIA) system with a measured limit of detection of 0.09 ng/ml was developed. Using this CLEIA system, it was found that soluble CRT (sCRT) level in serum samples from 58 lung cancer patients was significantly higher than that from 40 healthy individuals (only 9 were detectable, $P < 0.0001$). Among them, serum sCRT in the small cell lung cancer was lower than that in adenocarcinoma ($P = 0.0085$), while both were lower than that in the squamous cell carcinoma ($P = 0.013$, $P = 0.0012$, respectively). Moreover, it was found that sCRT in sera from the patients after chemotherapy was higher than that from the patients without chemotherapy ($P = 0.042$). Further study by immunohistochemistry showed that CRT was also highly expressed in the cytoplasm and on the membrane of the lung cancer cells, while there was a trace amount of CRT expression in normal lung cells. Correspondingly, the expression level of CRT on lung cancer cell membrane was associated with the tumor pathological grade. This study demonstrates that sCRT concentration in sera of lung cancer patients is higher than that in sera of healthy individuals, and CRT expression level on lung cancer cell membrane is associated with tumor pathological classification and grade. These findings suggest that CRT may be used as a biomarker in lung cancer prediction and diagnosis.

Keywords Calreticulin · Immune escape · Chemiluminescent enzyme immunoassay · Immunohistochemistry · Lung cancer

Abbreviations

CRT	Calreticulin
CLEIA	Chemiluminescent enzyme immunoassay
IHC	Immunohistochemistry

Introduction

Lung cancer is the leading cause of cancer-related mortality worldwide. Approximately 1.4 million deaths and 1.6 million new cases are reported each year [1]. Some tumor markers have been extensively studied in lung cancer, e.g., cytokeratin 19 fragment (CYFRA 21-1), carcinoembryonic

R. Liu, J. Gong and J. Chen contributed equally to the work.

R. Liu · J. Gong · Q. Li · C. Song · Y. Li · Z. Liu · Y. Dong · L. Chen (✉) · B. Jin (✉)
Department of Immunology, State Key Laboratory of Cancer Biology, Fourth Military Medical University, Xi'an 710032, China
e-mail: chenlh@fmmu.edu.cn

B. Jin
e-mail: immu_jin@fmmu.edu.cn

J. Chen
Department of Traditional Chinese Medicine, Xijing Hospital, Fourth Military Medical University, Xi'an 710032, China

J. Zhang
Department of Respiratory Medicine, Xijing Hospital, Fourth Military Medical University, Xi'an 710032, China

antigen (CEA), and squamous cell carcinoma (SCC) antigen; also, tissue polypeptide antigen (TPA) was used in the diagnosis of non-small cell lung cancer (NSCLC); neuron-specific enolase (NSE) was used to diagnose small cell lung cancer (SCLC) [2, 3]. Although these tumor makers for diagnosis in lung cancers exist, new methods for early diagnosis of lung cancer must be investigated.

In 1974, CRT was isolated from the sarcoplasmic reticulum (SR) of rabbit muscle. Further studies revealed that it was a major Ca^{2+}-binding protein in the endoplasmic reticula (ER) lumen [4]. After chemotherapies with anthracyclins (dutriomycin), CRT translocated from the ER to the cytosol, then subsequently to the cell surface. Previous experiments demonstrated that surface CRT can serve as an "eat me" signal [5] and induce the immunogenic tumor cell death [6–8]. Additionally, CRT exposure determines the engulfment of dying tumor cells by specific DC subsets [8]. Thus, CRT exposure plays important roles in tumor immunity.

There have been reports on the association between CRT expression level and various diseases [9–17]. It has been detected that there were higher levels of sCRT in the sera of patients with autoimmune disease such as rheumatoid arthritis and systemic lupus erythematosus [9]. In cancers, sCRT has been detected in sera of liver cancer patients [10] and in the urine of bladder cancer patients [11, 12]. In gastric cancer, it has been found that positive immunohistochemical staining of CRT was correlated with high microvessel density, lymph node spread, and poor patient survival [13]. Further, CRT was also found to be differentially expressed in colorectal cancer [14] and breast cancer [15, 16]. As to lung cancer, it has been reported that decreased CRT expression in lung cancer cell lines was associated with an increased rate of proliferation of lung cancer cells [17], which indicated the potential application of CRT in diagnosis and therapy of lung cancer. Recently, Soroush Merchant's group found that the surface expression of CRT was highly increased after 1 h Photofrin™ -photodynamic therapy (PDT) treatment in Lewis lung carcinoma (LLC) cells [18]. To further study the expression pattern and function of CRT in lung cancer, six clones of mouse anti-CRT mAbs were cloned and characterized. These six clones of mouse anti-CRT mAbs were used to develop a CLEIA system. Using this CLEIA system, serum CRT level in lung cancer patients was discovered to be significantly higher than that in healthy individuals. Moreover, the evaluation of the expression level of CRT in lung cancer tissues by immunohistochemical staining discovered that CRT expression level was correlated with clinic pathological parameters of lung cancer patients. These results suggested that CRT may be a novel prognostic biomarker in lung cancer and may serve as a new prospective therapeutic target for lung cancer.

Materials and methods

Samples from patients and healthy subjects

In 2010, 58 lung cancer patients (16 women and 42 men) were interviewed and selected from the Respiration Department of Xijing Hospital, Xi'an, China. With their permission, peripheral blood was collected. Ages ranged from 25 to 75 (median age, 57 years). Forty volunteers from the freshman Class of 2010 at Fourth Military Medical University (FMMU) were given physical examinations by the Outpatient Center of FMMU. Healthy serum samples were collected from them and processed within 18 h after collection. The serum samples were then stored at −20°C until the time to be used. Commercially paraffin-embedded microarrays (LC811) were purchased from Alenabiochnologies (Alenabio Technologies, Xi'an, China), which contained 80 lung cancer tissues of 80 different lung cancer patients and 10 normal lung tissues from 10 healthy individuals. The pathological types of the 80 lung cancer tissues were comprised of 17 squamous cell carcinoma, 26 small cell lung cancers, and 37 adenocarcinoma, which contained 12 alveolar cell carcinoma. The combined 90 samples (26 women and 64 men) ranged in ages from 16 to 77 (median age of 53). The final diagnosis of the lung cancer patients was made histologically on surgically excised tissues using WHO criteria. The definitions of pathology grades follow: G1—well differentiated; G2—moderately differentiated; G3—poorly differentiated; G4—undifferentiated; and Gx—unknown and unevaluated degree of differentiation. As previously mentioned, the use of all clinical materials was obtained with written informed consent and approved by the Institutional Research Ethics Committees.

Production of mouse mAbs to recombinant CRT/39–272

Complete Freund's adjuvant was mixed with 20 μg of rCRT/39–272 antigen [9]. Female BALB/c mice (6 weeks old) were immunized at day 0 by subcutaneous (s.c.) injection. After 3 weeks, the mice were subsequently immunized again with 20 μg protein in incomplete Freund's adjuvant by s.c. After another 3-week interval, the third immunization was made using 20 μg protein by intraperitoneal (i.p.) injection. Seven days after the last immunization, mice were bled from the caudal vein, and the serum titers were determined by indirect ELISA. The immunized mice with high serum titers were boosted with 50 μg antigen by i.p. injection. Three days later, their spleens were removed aseptically. Then, the splenocytes and Sp2/0 murine myeloma cells were fused in the presence of polyethylene glycol (MW4000; Merck, Darmstadt,

Germany). The positive hybrids were selected by ELISA and subcloned five times using the limiting dilution method. Mouse mAbs were produced from female BALB/c mice in which hybridoma cells had been i.p. injected. Immunoglobulin class and subclass determination of the mAbs were performed using a mouse mAb isotyping kit (Sigma, St. Louis, MO, USA) following the manufacturer's recommendations.

Sandwich ELISA

Six positive hybridoma clones secreting mouse mAbs against rCRT/39-272 were obtained and named as FMU-CRT 2, 8, 10, 17, 20, and 24, respectively. A portion of 100 μl FMU-CRT 2, 8, 10, 17, 20, and 24 (10 μg/ml in coating buffer) was added to each well of the ELISA plate (Corning-Costar, Corning, NY) and incubated overnight at 4°C. After extensive washing with PBS containing 0.1% (v/v) Tween-20 (PBS/Tween), every well was blocked with 200 μl PBS containing 10% calf serum for 1 h at 37°C. After washing again, standard rCRT/39–272 was serially diluted with dilution buffer and 100 μl/well standards were added to the wells, respectively. After incubation for 1 h at 37°C and 3 washings, the wells were reacted with FMU-CRT 2, 8, 10, 17, 20, and 24 conjugated with HRP as a detecting antibody that was diluted 1:500 in dilution buffer, respectively. The plate was incubated for 1 h at 37°C with 3 washings before 100 μl/well of substrate solution containing TMB was added. Next, the plate was incubated for 25 min at room temperature in a dark chamber. The reaction was subsequently quenched with 2 M sulfuric acid (50 μl/well), and the absorbance at 450 nm was measured with a microplate reader (Bio-Rad, Hercules, CA).

Establishment of the CLEIA kit for sCRT

The white opaque 96-flat-bottomed well plates (Greiner, Germany) were coated with FMU-CRT-17 mAb (10 μg/ml) in coating buffer and incubated at 4°C overnight. After 3 washings with washing buffer, free binding sites of the wells were blocked with 200 μl/well and PBS containing 10% calf serum for 1 h at room temperature. Afterward, 100 μl/well rCRT/39–272 which was serially diluted with dilution buffer was added. Plates were incubated at 37°C for 1 h with 3 washings. Then, the wells were reacted with a detecting antibody FMU-CRT-8 mAb (100 μl/well) that had been conjugated with HRP and diluted (1:3,000) in dilution buffer. After incubation at 37°C for 1 h and 3 more extensive washings, the chemiluminescent substrates (mixture of SuperSignal ELISA femto luminol enhancer solution and SuperSignal ELISA femto stable peroxide solution, 100 μl/well) were added into the plates in a ratio of 1:1. The chemiluminometric signal generated from the HRP luminol H_2O_2 system was emitted and analyzed at the Alpha InfoTech FluorChem FC2 Imaging System (Alpha Innotech, USA). The standard protein and all clinical samples were measured in duplicate.

Flow cytometry

The binding of mAbs to the CRT molecules on the cell surface was determined by flow cytometry analysis (FCM). After blocking with normal goat serum (10%), Jurkat cells were incubated with FMU-CRT 2, 8, 10, 17, 20, and 24 mAbs, respectively. Mouse anti-staphylococcal enterotoxin (anti-SED) mAb which prepared and identified previously was used as the negative control [19]. After 2 washings in Dulbecco's PBS (DPBS), the cells were suspended in DPBS containing a working dilution of fluorescein isothiocyanate (FITC) labeled goat anti-mouse IgG (BioLegend, USA) and were incubated at 4°C for 30 min. The cells were washed, fixed, and then analyzed on a fluorescence-activated cell sorter (FACScan) cytometer (Elite ESP, Miami, FL, USA).

Western blot analysis

A total of 10 ug of rCRT/39-272 protein was electrophoresed on 12% sodium dodecyl sulfate–polyacrylamide electrophoresis gel and transferred to nitrocellulose membranes (Amersham, Little Chalfont, UK). Membranes were blocked and incubated with FMU-CRT 2, 8, 10, 17, 20, and 24 (1:1,000 mAb ascites) at 4°C overnight, respectively. Normal mouse IgG was used as the negative control. After 4 washings, the membranes were reacted with HRP-labeled goat anti-mouse IgG for 1 h at room temperature. After 4 washings, enhanced chemiluminescence reagent (Roche, Indianapolis, IN, USA) was applied to the membranes that were then exposed to the Alpha Innotech FluorChem FC2 Imaging System (Alpha Innotech, USA) according to the manufacturer's instructions.

Immunohistochemistry

A mixture of CHO cells and Jurkat cells was fixed in 4% paraformaldehyde for 24 h followed by dehydration in gradient ethanol and was made into a paraffin block. Then, the paraffin block was cut at 5 μm thickness and mounted on gelatin-coated slides. The slices were de-waxed, hydrated, and incubated in peroxidase inhibitor for 30 min to remove endogenous peroxidase. After blocking with diluted goat serum (Sigma, USA), they were dipped into mouse FMU-CRT 2, 8, 10, 17, 20, and 24 mAbs (diluted to 1:2,500) at 4°C overnight. Mouse anti-SED mAb was applied as the negative control. After 3 washings in PBS, the slices were dipped into HRP-conjugated goat

anti-mouse IgG (Abcam, Cambridge, UK) for 30 min at room temperature. Antigen–antibody complexes were incubated with DAB chromogen and observed. Sections were counterstained with Mayer's hematoxylin for 2 min, dehydrated through gradient ethanol, cleared in dimethyl benzene, then mounted and examined using light microscopy (Olympus, Tokyo, Japan). The percentage of positive cells was divided into five grades (percentage scores): <10% (0), 10–25% (1), 26–50% (2), 51–75% (3), and >75% (4). The intensity of the staining was divided into four grades (intensity scores): no staining (0), light brown (1), brown (2), and dark brown (3). CRT staining positivity was determined using the following formula: overall score = percentage score × intensity score. An overall score of ≤1, >1 to ≤3, >3 to ≤6, and >6 was defined as negative, weak positive, moderate positive, and strong positive, respectively.

Statistical analysis

Each experiment was performed independently 3 times with similar results, and one representative experiment was presented. All statistical analyses were performed using the statistical software package (SPSS for Windows, version 12.0; SPSS Inc; Chicago, IL). The differences of the three groups of sCRT were analyzed using the one-way ANOVA and the post hoc tests were LSD. Fitting of the curves were performed with the GraphPad Prism software (version 4.0 for Windows, GraphPad Software, San Diego, CA). The experimental curve was estimated by linear regression.

Results

Preparation and identification of mAbs to rCRT/39–272

Six positive hybridoma clones secreting mouse mAbs against rCRT/39-272 were obtained and named as FMU-CRT 2, 8, 10, 17, 20, and 24, respectively. The mouse Ig isotypes of FMU-CRT 2, 8, 10, and 24 mAbs were IgG1, while the isotypes of FMU-CRT 17 and 20 mAbs were IgM (Table 1).

Flow cytometric analysis

The FCM analysis showed that FMU-CRT 10, 17, 20, and 24 could recognize the natural membrane CRT molecule expressed on the human T cell lymphoblast-like line Jurkat cells, which has been proven to express CRT on membrane [20]. The positive percentages were 37.95, 38.76, 39.51, and 28.21%, respectively. In contrast, FMU-CRT 2 and 8 displayed little reactivity, 2.96 and 4.12%, respectively (Fig. 1A).

Table 1 Characterization of anti-CRT monoclonal antibodies

Clone number	Class/subclass/type	Ascites titers	WB	FCM	IHC
FMU-CRT-2	IgG1/k	10^{-7}	+	−	++
FMU-CRT-8	IgG1/k	10^{-6}	+	−	+
FMU-CRT-10	IgG1/k	10^{-6}	+	+	+
FMU-CRT-17	IgM/k	10^{-7}	+	+	+
FMU-CRT-20	IgM/k	10^{-4}	+	+	−
FMU-CRT-24	IgG1/k	10^{-5}	+	+	−

FCM flow cytometry analysis, *IHC* immunohistochemistry, *WB* Western blot, *IgG* immunoglobulin G, *IgM* immunoglobulin M, ++ strongly positive, + positive, − negative

Western blot analysis

FMU-CRT 2, 8, 10, 17, 20, and 24 can probe the rCRT/39-272 molecule that is 46 kDa by Western blot analysis, while control antibody displayed negative reactivity (Fig. 1B).

Immunohistochemistry

The immunohistochemistry results showed that FMU-CRT-2 could recognize CRT-reactive substances located in the Jurkat cells' paraffin block slices, which were observed by strong DAB staining in the cytoplasms (Fig. 1C.a). In comparison with FMU-CRT-2, FMU-CRT 8, 10, and 17 could also recognize CRT-reactive substances located in Jurkat cells moderately (Fig. 1C.b). FMU-CRT 20, 24, and control antibody showed negative results (Fig. 1C.c, d).

Establishment of the sandwich ELISA system for detecting sCRT

In order to determine the optimum combination of the sandwich ELISA system, each of the aforementioned six mAbs was labeled with HRP and then utilized as either the coating or a detection antibody. The data shown in Fig. 2A indicated that the highest number of the OD 450 nm absorbance was obtained when FMU-CRT-17 mAb was used as the coating antibody, and HRP-labeled FMU-CRT-8 mAb was used as the detection antibody. Compared with this pairwise, other pairwises showed lower absorbance. As expected, low or no counts were observed when the same mAb was used as both the capture and detection antibody (Fig. 2A). Further study by double diluted rCRT to make standard curves confirmed that FMU-CRT-17 mAb as the coating antibody and HRP-labeled FMU-CRT-8 mAb as the detection antibody were the most satisfactory combination (Fig. 2B). The linear dynamic range was between 6.25 and 200 ng/ml. The detection limitation of sCRT was 0.39 ng/ml.

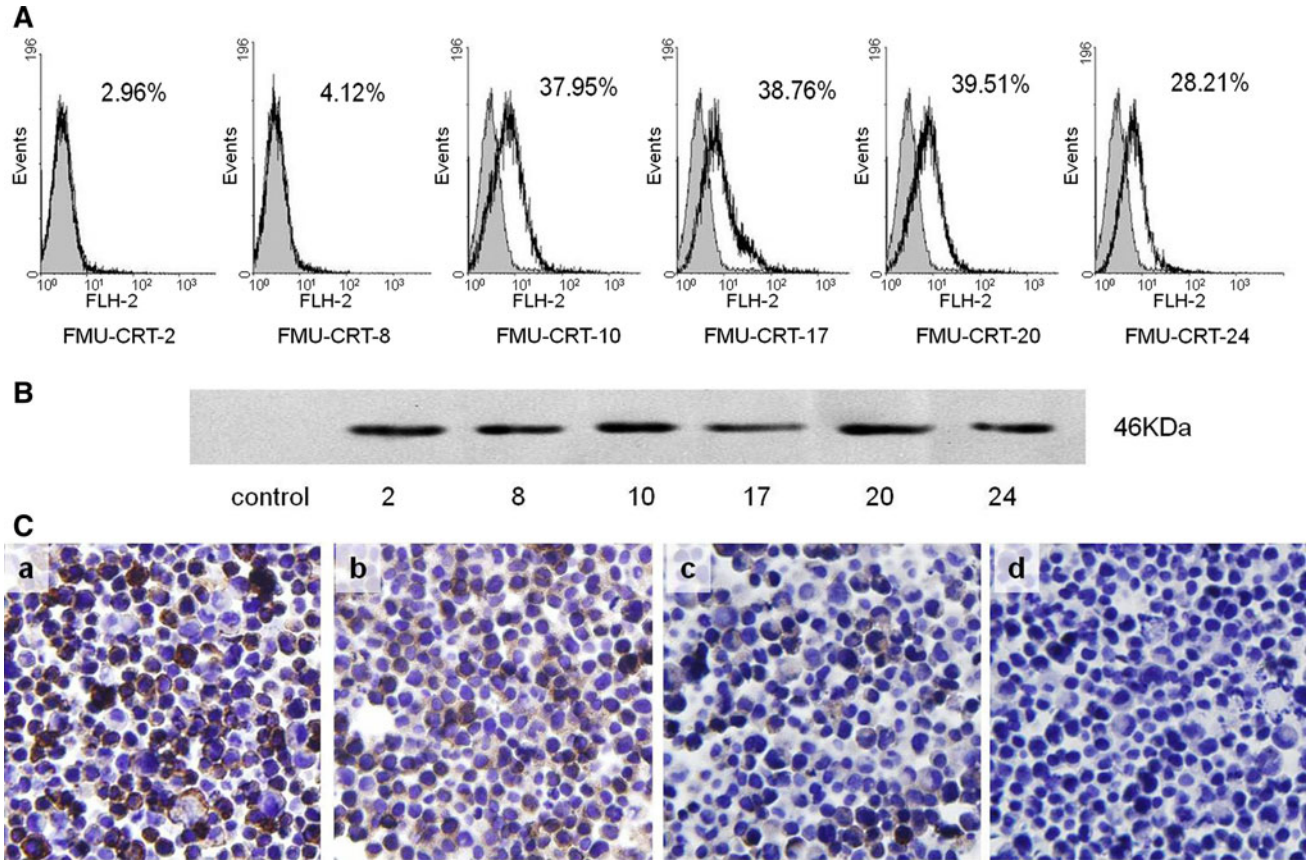

Fig. 1 Identification and characterization of FMU-CRT 2, 8, 10, 17, 20, and 24 mAbs. **A** Reactivity of FMU-CRT 2, 8, 10, 17, 20, and 24 with membrane CRT identified by flow cytometric analysis. Jurkat cells were stained with the control mAb (*gray histogram*) or FMU-CRT 2, 8, 10, 17, 20, 24 (*solid line*), respectively. **B** Western blot analysis showed FMU-CRT 2, 8, 10, 17, 20, and 24 could probe the rCRT molecule, control antibody displayed negative reactivity. **C** Identification of FMU-CRT 2, 8, 10, 17, 20, and 24 mAbs by immunohistochemistry. The paraffin sections of a mixture of CHO cells (CRT negative) and Jurkat cells (CRT positive) were stained with FMU-CRT 2, 8, 10, 17, 20, 24, and the control mAbs, respectively, and visualized by incubation with DAB chromogen. Among these mAbs, FMU-CRT-2 (**a**), FMU-CRT-8 (**b**), FMU-CRT-10, and FMU-CRT-17 (*data not shown*) could be used in immunohistochemistry. FMU-CRT-20 (**c**), FMU-CRT-24 (*data not shown*), and the control mAb (**d**) were immunoreactive-negative. ×400

Optimization of CLEIA for detecting sCRT

According to the results obtained from the sandwich ELISA system above, a sandwich sCRT CLEIA system was established by using FMU-CRT-17 mAb as the coating antibody and HRP-conjugated FMU-CRT-8 mAb as the detection antibody. To further improve the sensitivity of CLEIA, FMU-CRT-17 (IgM) mAb was purified by gel filtration chromatography column (superdex^{TM} 200) and FMU-CRT-8 (IgG1) mAb was purified by ion-exchange chromatography column (Q Sepharose Fast Flow), respectively. It is well known that optimization of the appropriate dilution of HRP conjugate is one of the key factors determining the sensitivity and working range of CLEIA [21]. To reduce background noise and to obtain maximized sensitivity in sCRT CLEIA, a series of dilution ratios (1:600, 1:800, 1:1,500, and 1:3,000) of HRP-labeled FMU-CRT-8 mAbs were tested. Finally, the dilution ratio of HRP-labeled FMU-CRT-8 mAb 1:3,000 and the concentration of FMU-CRT-17 mAb of 10 μg/ml were selected. Standard curves were obtained by plotting relative light units (RLU) against the analyte concentration of CRT (Fig. 2C). The detectable limitation of sCRT was improved from 0.39 ng/ml to 0.09 ng/ml by CLEIA.

Determination of sCRT levels in sera of patients with lung cancer

Using the sCRT CLEIA system, serum level of sCRT in 9 individuals among the 40 healthy volunteers could be detected, which could not be detected by ELISA system previously. The level of sCRT in lung cancer patients ($n = 58$, median = 0.747 ng/ml, inter quartile range

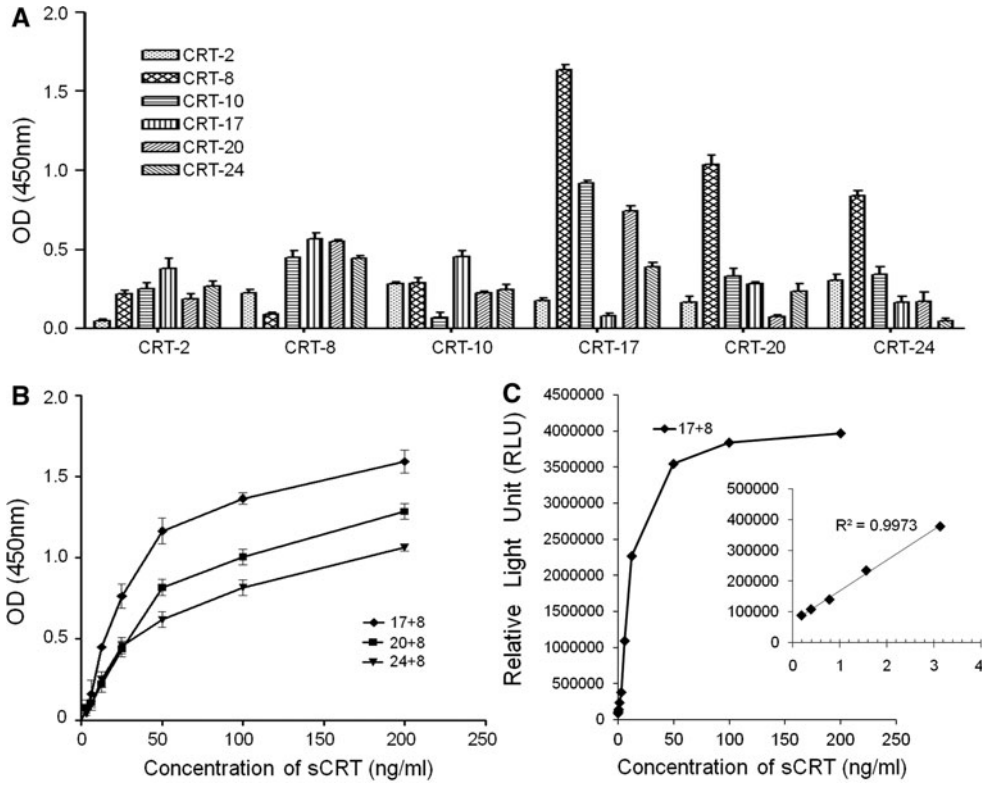

Fig. 2 Establishment of the CLEIA system with FMU-CRT-17 mAb as coating antibody and HRP-conjucted FMU-CRT-8 mAb as detection antibody to detect soluble CRT. **A** Each of the six mAbs was used as coating antibody or as HRP-labeled detection antibody. The optical density (OD) 450 nm absorbance was detected for each antibody combination using sCRT concentration at 100 ng/ml. *Histograms* represented means of triplicate determinations (*bars* show mean with SD). **B** Standard calibration curves of sandwich ELISA with three combinations of anti-sCRT mAbs. Plotted values were obtained with 6.25, 12.5, 25, 50, 100, and 200 ng/ml rCRT by sandwich ELISA as described in materials and methods. Line graph is means of triplicate determinations. **C** Standard calibration curves of sCRT CLEIA with FMU-CRT-17 as coating mAb and HRP-labeled FMU-CRT-8 as detection mAb. Plotted values were obtained with 0.19, 0.39, 0.78, 1.56, 3.125, 6.25, 12.5, 25, 50, 100, and 200 ng/ml rCRT. The inset was the amplification of 0.19–3.125 ng/ml rCRT

(IQR) = 1.719 ng/ml, maximum = 5.766 ng/ml) was significantly higher than that in healthy individuals ($P < 0.0001$) by CLEIA system (Fig. 3A). According to the pathological type of lung cancer, we analyzed the serum sCRT level of 58 patients with adenocarcinoma ($n = 19$, median = 1.06 ng/ml, IQR = 1.147 ng/ml, maximum = 3.24 ng/ml), squamous cell carcinoma ($n = 18$, median = 1.365 ng/ml, IQR = 1.995 ng/ml, maximum = 5.766 ng/ml), and SCLC ($n = 21$, median = 0.436 ng/ml, IQR = 0.617 ng/ml, maximum = 2.594 ng/ml). The results showed that sCRT level in sera of the SCLC patients was significantly lower than that in the other two types (Fig. 3B). Moreover, sCRT level in sera of the lung cancer patients with chemotherapy ($n = 46$, median = 1.042 ng/ml, IQR = 1.327 ng/ml) was higher than that of the patients without chemotherapy ($n = 12$, median = 0.616 ng/ml, IQR = 0.859 ng/ml, Fig. 3C), which indicated that the chemotherapeutic agents may induce translocation and secretion of CRT in lung cancer cells.

High expression level of CRT in human lung cancer tissues

It has been reported that when tumor cells undergo immunogenic apoptosis, CRT could transfer from ER membrane to the cell surface [22]. In our study, CRT was found to localize not only in the cytoplasm but also on the membrane of the lung cancer cells (Fig. 4). Furthermore, with the increasing pathological grade of malignant tumor, the expression of CRT on the membrane of the cancer cells correspondingly increased (Table 2). From G1 to G3, the percentage of positive cases with CRT expression on the cytomembrane in adenocarcinoma tissues ($n = 24$) was rising correspondingly (0, 25 and 63.6%), while the percentage of CRT positive cases in the cytoplasm was reduced correspondingly (100, 75, and 36.4%). The positive CRT only expressed in the cytoplasm of G1 and G2 squamous cell carcinoma tissues, but expressed both on the cytomembrane and in the cytoplasm of G3 squamous cell

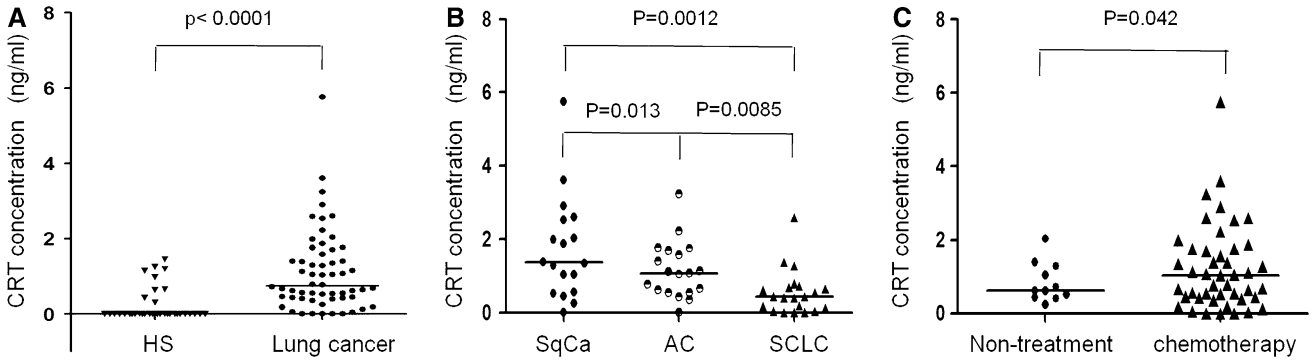

Fig. 3 Detection of soluble CRT in sera. Serum samples (not diluted) from patients were individually assayed for the presence of sCRT using CLEIA, and the results are expressed as CRT concentrations (ng/ml). **A** The level of the sCRT in sera of patients with lung cancer ($n = 58$) and that of healthy human subjects (HS, $n = 40$). **B** The level of the sCRT in sera of three different pathological types of patient groups. SqCa: Squamous cell carcinoma ($n = 18$); SCLC: small cell lung cancer ($n = 21$); AC: adenocarcinoma ($n = 19$). **C** The level of the sCRT in sera of patients without ($n = 12$) and with chemotherapy ($n = 46$). All the mean values were shown by *horizontal lines*

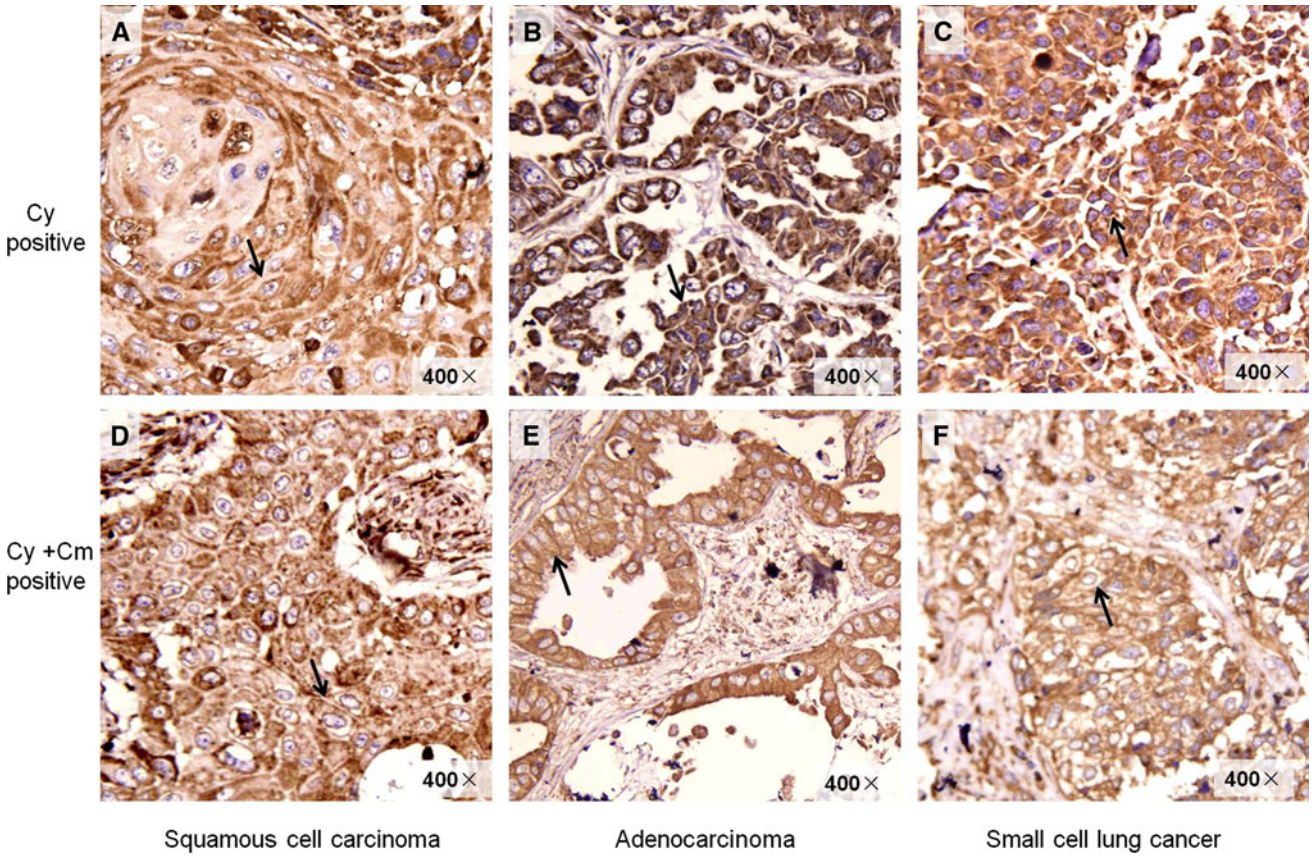

Fig. 4 Different expression profile of CRT in lung cancer tissues. **A** Squamous cell carcinoma tissue, G1, CRT expression was found predominantly Cy positive. **B** Adenocarcinoma tissue, G1, Cy positive. **C** SCLC, Cy positive. **D** Squamous cell carcinoma tissue, G3, CRT expression was gradually translocated to the Cm. **E** Adenocarcinoma, G3, Cy and Cm positive. **F** SCLC, Cy and Cm positive. The *arrows* in **A**, **B** and **C** represent the positive CRT expression in Cy. The *arrows* in **D**, **E** and **F** represent the positive CRT expression in Cm. *Cy* cytoplasm, *Cm* cytomembrane. ×400

carcinoma tissues, the positive proportion being 29%. However, it was surprising that 46.1% of the tissues of small cell lung cancer (G4) did not express CRT and only 11.5% of them expressed CRT on both of the cytomembrane and cytoplasm (Table 2). The concrete mechanisms need further clarification.

Table 2 Expression of CRT in different pathological types of lung cancer

Type	Pathological grade	Cases	Positive (*n*%)		Negative (*n*%)
			Cy	Cy + Cm	
Adenocarcinoma	G1	6	6 (100)	0	0
	G2	8	6 (75.0)	2 (25.0)	0
	G3	11	4 (36.4)	7 (63.6)	0
Alveolar cell carcinoma		12	11 (91.6)	1 (8.3)	0
Squamous cell carcinoma	G1	4	4 (100)	0	0
	G2	6	6 (100)	0	0
	G3	7	5 (71.4)	2 (28.6)	0
Small cell lung cancer	G4	26	11 (42.3)	3 (11.5)	12 (46.1)
Normal lung tissue		10	0	0	10 (100)
Total		90			

Cy cytoplasm, *Cm* cytomembrane

Discussion

CRT was given the name HACBP (high-affinity calcium-binding protein) in 1974. Until 1989, the cDNA encoding this Ca^{2+}-binding protein was isolated. In order to acknowledge both its Ca^{2+}-binding properties and its localization to the ER lumen, HACBP was renamed CRT [4]. However, now it is recognized as a multifunctional protein not only expressed in the cytoplasm but also on the cellular surface, in serum, and in the extracellular matrix [20]. On these different locations, CRT has been shown to be required for antigen processing and presentation for the adaptive immune response [23, 24], phagocytosis of apoptotic cells [5], cell adhesion, migration [25–27], and cellular proliferation [27]. Because of CRT's role in these biological activities, this ER-resident protein is emerging as a critical mediator of physiological and pathological processes. More importantly, it has been found that the process of immune-mediated destruction of cancer cells is dependent on the cell surface expression of CRT [8, 22–24, 28–30]. The translocation and exposure of CRT and the uptake of CRT-expressing cancer cells by dendritic cells [24, 31] dictate the immunogenicity of tumor cell death [8, 23, 29].

It has been reported that CRT could be a biomarker in bladder cancer [11]. The measurable dynamic range of the ELISA system used in that paper was from 0.5 to 1,000 ng/ml, but the urinary CRT of non-bladder cancer group was <0.5 ng/ml [11]. Therefore, there is a limitation for the detection of sCRT. Another sandwich ELISA system previously reported could only detect sCRT in sera from 23.3% RA patients and 21.9% SLE patients and could not detect sCRT in any of the 48 serum samples from healthy subjects [9]. Thus, new detecting systems for measuring sCRT sensitively need to be developed further.

CLEIA is an enhanced chemiluminescent immunoassay with high sensitivity, wide dynamic range, and suitability for miniaturization. It has been reported that the sensitivity of the chemiluminescent reaction often exceeds that of radioactivity assays [21]. Based on the sandwich ELISA system, a CLEIA system was developed for detecting serum sCRT with the measured limit of detection (LOD) 0.09 ng/ml. Using this CLEIA system, it has been found that all the serum sCRT of lung cancer patients and 9 out of 40 healthy subjects were detectable.

The association between CRT expression and various diseases has been previously reported. A higher amount of CRT was found in the urine samples of patients with bladder cancer, and CRT was proposed as a biomarker in bladder cancer [11]. It has been reported that over expression of CRT or CRT fragments in tumor cell lines enhanced in migration and invasion [32, 33]. In gastric cancer, positive immunohistochemical staining of CRT was correlated with high microvessel density, lymph node spread, poor patient survival, and enhanced gastric cancer cell proliferation and migration [13]. It was observed that a potential correlation of CRT over expression with axillary lymph node metastasis in breast cancer patients [15]. However, other studies have reported alternative roles for CRT. In neuroblastoma, positive immunohistochemical staining for CRT was correlated with better prognosis and patient survival [34]. In lung cancer cell lines, it was reported that the reduction in expression of CRT was associated with an increased rate of proliferation [17]. In this study, it has been found that sCRT level in sera of lung cancer patients is significantly higher than that in the healthy individuals. Corresponding to this, the lung cancer tissues were also shown positive CRT immnohistochemical staining while normal lung tissues were negative. The percentage of positive CRT immunostaining on membrane of lung cancer cells increased as the tumor histology became differentiated.

Since lung cancer of different histological types shows various characteristics in invasion, metabasis, prognosis, and reaction to chemotherapy or radiotherapy, the expression level of sCRT in sera of different histological type

lung cancer patients was detected. It was observed that sCRT levels in sera of adenocarcinoma patients (median = 1.04 ng/ml) and squamous cell carcinoma patients (median = 1.35 ng/ml) were higher than that in the small cell lung cancer patients (median = 0.42 ng/ml). Corresponding to this, almost all of the adenocarcinoma and squamous cell carcinoma tissues expressed CRT, while only 14 out of 26 (53.8%) small cell lung cancer did. Although the tissue and serum samples in this study were not from the same patients, sCRT levels in sera of lung cancer patients of different histological types were consistent with the CRT membrane expression of lung cancer patients of different histological types. So the results of our study suggest that the expression profile of CRT is associated with the pathological type of lung cancers.

It has been reported that the translocation of CRT is induced upon treatment for tumor cells with anthracyclins, oxaliplatin, and ionizing irradiation, but other cell death inducers targeting ER (tunicamiycin and brefeldin), mitochondria (arsenite, betulinic acid, and C2 ceramide), or DNA (Hoechst 33342, camptothecin, etoposide, and mitomycin C) fail to induce CRT exposure and immunogenic cell death [23]. In this research, sCRT level in sera of patients after chemotherapy was higher than that of patients without chemotherapy. This is at least in part consistent with the previous report.

In conclusion, CRT was observed to be overexpressed in lung cancer tissues. Moreover, the percentage of positive CRT immunostaining on membrane of lung cancer cells increased as the tumor histology became differentiated, thus demonstrating that sCRT expression increased in sera of lung cancer patients and correlated with the lung cancer pathologic type. The low expression of CRT in the cytoplasm, on the membrane, and in sera in small lung cancer may represent a new mechanism of immune escape and the increasing expression level of CRT on the membrane may indicate new therapy strategies for high malignant lung cancers.

Acknowledgments We thank Institute of Biology and Medical Sciences Soochow University (Suzhou, China) for the antigen rCRT39/272. This work was supported by the National Natural Science Foundation of China (30972683 and 31070794).

Conflict of interest The authors declare that they have no conflict of interest.

References

1. Jemal A, Center MM, DeSantis C, Ward EM (2010) Global patterns of cancer incidence and mortality rates and trends. Cancer Epidemiol Biomarkers Prev 19(8):1893–1907
2. Molina R, Auge JM, Bosch X, Escudero JM, Vinolas N, Marrades R, Ramirez J, Carcereny E, Filella X (2009) Usefulness of serum tumor markers, including progastrin-releasing peptide, in patients with lung cancer: correlation with histology. Tumour Biol 30(3):121–129
3. Ramalingam SS, Owonikoko TK, Khuri FR (2011) Lung cancer: new biological insights and recent therapeutic advances. CA Cancer J Clin 61(2):91–112
4. Johnson S, Michalak M, Opas M, Eggleton P (2001) The ins and outs of calreticulin: from the ER lumen to the extracellular space. Trends Cell Biol 11(3):122–129
5. Gardai SJ, McPhillips KA, Frasch SC, Janssen WJ, Starefeldt A, Murphy-Ullrich JE, Bratton DL, Oldenborg PA, Michalak M, Henson PM (2005) Cell-surface calreticulin initiates clearance of viable or apoptotic cells through trans-activation of LRP on the phagocyte. Cell 123(2):321–334
6. Tongu M, Harashima N, Yamada T, Harada T, Harada M (2010) Immunogenic chemotherapy with cyclophosphamide and doxorubicin against established murine carcinoma. Cancer Immunol Immunother 59(5):769–777
7. Perez CA, Fu A, Onishko H, Hallahan DE, Geng L (2009) Radiation induces an antitumour immune response to mouse melanoma. Int J Radiat Biol 85(12):1126–1136
8. Obeid M, Panaretakis T, Joza N, Tufi R, Tesniere A, van Endert P, Zitvogel L, Kroemer G (2007) Calreticulin exposure is required for the immunogenicity of gamma-irradiation and UVC ?tul?> light-induced apoptosis. Cell Death Differ 14(10): 1848–1850
9. Hong C, Qiu X, Li Y, Huang Q, Zhong Z, Zhang Y, Liu X, Sun L, Lv P, Gao XM (2010) Functional analysis of recombinant calreticulin fragment 39–272: implications for immunobiological activities of calreticulin in health and disease. J Immunol 185(8):4561–4569
10. Chignard N, Shang S, Wang H, Marrero J, Brechot C, Hanash S, Beretta L (2006) Cleavage of endoplasmic reticulum proteins in hepatocellular carcinoma: detection of generated fragments in patient sera. Gastroenterology 130(7):2010–2022
11. Kageyama S, Isono T, Matsuda S, Ushio Y, Satomura S, Terai A, Arai Y, Kawakita M, Okada Y, Yoshiki T (2009) Urinary calreticulin in the diagnosis of bladder urothelial carcinoma. Int J Urol 16(5):481–486
12. Kageyama S, Isono T, Iwaki H, Wakabayashi Y, Okada Y, Kontani K, Yoshimura K, Terai A, Arai Y, Yoshiki T (2004) Identification by proteomic analysis of calreticulin as a marker for bladder cancer and evaluation of the diagnostic accuracy of its detection in urine. Clin Chem 50(5):857–866
13. Chen CN, Chang CC, Su TE, Hsu WM, Jeng YM, Ho MC, Hsieh FJ, Lee PH, Kuo ML, Lee H, Chang KJ (2009) Identification of calreticulin as a prognosis marker and angiogenic regulator in human gastric cancer. Ann Surg Oncol 16(2):524–533
14. Alfonso P, Nunez A, Madoz-Gurpide J, Lombardia L, Sanchez L, Casal JI (2005) Proteomic expression analysis of colorectal cancer by two-dimensional differential gel electrophoresis. Proteomics 5(10):2602–2611
15. Eric A, Juranic Z, Milovanovic Z, Markovic I, Inic M, Stanojevic-Bakic N, Vojinovic-Golubovic V (2009) Effects of humoral immunity and calreticulin overexpression on postoperative course in breast cancer. Pathol Oncol Res 15(1):89–90
16. Lwin ZM, Guo C, Salim A, Yip GW, Chew FT, Nan J, Thike AA, Tan PH, Bay BH (2010) Clinicopathological significance of calreticulin in breast invasive ductal carcinoma. Mod Pathol 23(12):1559–1566
17. Bergner A, Kellner J, Tufman A, Huber RM (2009) Endoplasmic reticulum Ca2+-homeostasis is altered in small and non-small cell lung cancer cell lines. J Exp Clin Cancer Res 28:25
18. Korbelik M, Zhang W, Merchant S (2011) Involvement of damage-associated molecular patterns in tumor response to photodynamic therapy: surface expression of calreticulin and

high-mobility group box-1 release. Cancer Immunol Immunother 60(10):1431–1437
19. Gong J, Zhu C, Zhuang R, Song C, Li Q, Xu Z, Wei Y, Yang K, Yang A, Chen L, Jin B (2009) Establishment of an enzyme-linked immunosorbent assay system for determining soluble CD96 and its application in the measurement of sCD96 in patients with viral hepatitis B and hepatic cirrhosis. Clin Exp Immunol 155(2): 207–215
20. Gold LI, Eggleton P, Sweetwyne MT, Van Duyn LB, Greives MR, Naylor SM, Michalak M, Murphy-Ullrich JE (2010) Calreticulin: non-endoplasmic reticulum functions in physiology and disease. FASEB J 24(3):665–683
21. Liu F, Li Y, Song C, Dong B, Liu Z, Zhang K, Li H, Sun Y, Wei Y, Yang A, Yang K, Jin B (2010) Highly sensitive microplate chemiluminescence enzyme immunoassay for the determination of staphylococcal enterotoxin B based on a pair of specific monoclonal antibodies and its application to various matrices. Anal Chem 82(18):7758–7765
22. Panaretakis T, Kepp O, Brockmeier U, Tesniere A, Bjorklund AC, Chapman DC, Durchschlag M, Joza N, Pierron G, van Endert P, Yuan J, Zitvogel L, Madeo F, Williams DB, Kroemer G (2009) Mechanisms of pre-apoptotic calreticulin exposure in immunogenic cell death. EMBO J 28(5):578–590
23. Obeid M, Tesniere A, Ghiringhelli F, Fimia GM, Apetoh L, Perfettini JL, Castedo M, Mignot G, Panaretakis T, Casares N, Metivier D, Larochette N, van Endert P, Ciccosanti F, Piacentini M, Zitvogel L, Kroemer G (2007) Calreticulin exposure dictates the immunogenicity of cancer cell death. Nat Med 13(1):54–61
24. Tesniere A, Apetoh L, Ghiringhelli F, Joza N, Panaretakis T, Kepp O, Schlemmer F, Zitvogel L, Kroemer G (2008) Immunogenic cancer cell death: a key-lock paradigm. Curr Opin Immunol 20(5):504–511
25. Coppolino MG, Woodside MJ, Demaurex N, Grinstein S, St-Arnaud R, Dedhar S (1997) Calreticulin is essential for integrin-mediated calcium signalling and cell adhesion. Nature 386(6627):843–847
26. Orr AW, Pallero MA, Xiong WC, Murphy-Ullrich JE (2004) Thrombospondin induces RhoA inactivation through FAK-dependent signaling to stimulate focal adhesion disassembly. J Biol Chem 279(47):48983–48992
27. Nanney LB, Woodrell CD, Greives MR, Cardwell NL, Pollins AC, Bancroft TA, Chesser A, Michalak M, Rahman M, Siebert JW, Gold LI (2008) Calreticulin enhances porcine wound repair by diverse biological effects. Am J Pathol 173(3):610–630
28. Chaput N, De Botton S, Obeid M, Apetoh L, Ghiringhelli F, Panaretakis T, Flament C, Zitvogel L, Kroemer G (2007) Molecular determinants of immunogenic cell death: surface exposure of calreticulin makes the difference. J Mol Med 85(10):1069–1076
29. Obeid M, Panaretakis T, Tesniere A, Joza N, Tufi R, Apetoh L, Ghiringhelli F, Zitvogel L, Kroemer G (2007) Leveraging the immune system during chemotherapy: moving calreticulin to the cell surface converts apoptotic death from "silent" to immunogenic. Cancer Res 67(17):7941–7944
30. Tufi R, Panaretakis T, Bianchi K, Criollo A, Fazi B, Di Sano F, Tesniere A, Kepp O, Paterlini-Brechot P, Zitvogel L, Piacentini M, Szabadkai G, Kroemer G (2008) Reduction of endoplasmic reticulum Ca2+ levels favors plasma membrane surface exposure of calreticulin. Cell Death Differ 15(2):274–282
31. Zeng G, Aldridge ME, Tian X, Seiler D, Zhang X, Jin Y, Rao J, Li W, Chen D, Langford MP, Duggan C, Belldegrun AS, Dubinett SM (2006) Dendritic cell surface calreticulin is a receptor for NY-ESO-1: direct interactions between tumor-associated antigen and the innate immune system. J Immunol 177(6):3582–3589
32. Chao MP, Jaiswal S, Weissman-Tsukamoto R, Alizadeh AA, Gentles AJ, Volkmer J, Weiskopf K, Willingham SB, Raveh T, Park CY, Majeti R, Weissman IL (2010) Calreticulin is the dominant pro-phagocytic signal on multiple human cancers and is counterbalanced by CD47. Sci Transl Med 2(63):63ra94
33. Liu M, Imam H, Oberg K, Zhou Y (2005) Gene transfer of vasostatin, a calreticulin fragment, into neuroendocrine tumor cells results in enhanced malignant behavior. Neuroendocrinology 82(1):1–10
34. Hsu WM, Hsieh FJ, Jeng YM, Kuo ML, Chen CN, Lai DM, Hsieh LJ, Wang BT, Tsao PN, Lee H, Lin MT, Lai HS, Chen WJ (2005) Calreticulin expression in neuroblastoma: a novel independent prognostic factor. Ann Oncol 16(2):314–321